Available online at www.sciencedirect.com

ScienceDirect

Trans. Nonferrous Met. Soc. China 21(2011) 250−256

Transactions of Nonferrous Metals Society of China

www.tnmsc.cn

Microstructure characteristics and solidification behavior of thixomolded Mg-9%Al-1%Zn alloy

ZHANG You-fa[1], LIU Yong-bing[2], CAO Zhan-yi[2]

1. Jiangsu Key Laboratory of Advanced Metallic Materials, School of Materials Science and Engineering, Southeast University, Nanjing 211189, China;

2. Key Laboratory of Automobile Materials of Ministry of Education, School of Materials Science and Engineering, Jilin University, Changchun 130022, China

Received 24 March 2010; accepted 3 June 2010

Abstract: Experimental investigation and theoretical analysis of the microstructure of thixomolded AZ91D were carried out to comprehensively understand the morphology transformation of solid particles and the solidification behavior. Typical microstructure of thixomolded AZ91D is composed of α-Mg and β-$Mg_{17}Al_{12}$, characterized with α_{un}, α_{prim} and eutectic. Four kinds of α_{un} are classified according to the morphology and generation mechanism, such as spherical (α_1), irregular (α_2), entrapping liquid alloy inside (α_3) and entrapping pool inside (α_4). Under the effect of heating, shearing, collision, agglomeration or fragmentation, α_2 and α_4 can be the middle states of α_1 and α_3. Similarly, α_4 and α_3 can also break into α_2 and become α_1 at the end. Controlled by undercooling, α_{prim} nucleates and spherically grows within the remaining liquid alloy of thixomolded AZ91D until instability growth. The investigated microstructure was theoretically proved according to the analysis of Mg-Al binary phase diagram.

Key words: thixomolded AZ91D alloy; solid particle; solidification behavior

1 Introduction

Magnesium alloys, the lightest metallic materials in engineering application, are called as green engineering materials in the 21st century[1]. Thixomolding®, as the unique commercial technology of semisolid forming or semisolid processing (SSF/SSP), has been successfully used to manufacture high-quality and high-property magnesium products[2−4]. During the last 10 years, a great progress has been achieved in understanding the unique microstructure and mechanical properties of semisolid alloys. Among the topics of semisolid processing, the existence and transformation of non-dendritic solid particles were deeply researched[5−7]. Recrystallization of the deformed dendritic within the alloys was proposed to explain the transformation of the solid particles with increasing temperature[6−8]. According to the generation mechanism, the effects of microstructure on mechanical properties have been extensively investigated for thixomolded AZ91D alloy[4−5]. It was found that the volume fraction and morphology of solid particles had great influence on the properties. Low volume fraction and round shape were required to the good rheology and high properties, which was also shown by other researches[7, 9−10]. All the results displayed that the fraction, size and morphology of the non-dendritic solid particles have a great influence on the final microstructure and corresponding mechanical properties. However, the chemical composition, size and morphology evolutions of the non-dendritic solid particles have not been paid much attention to, and solidification behavior of the rest liquid alloy was always neglected in despite of the significant role of the liquid alloy[11]. HITCHCOCK et al[12] investigated the solidification behavior of the liquid in semisolid Al-7Si-0.6Mg slurry in the rheo-diecasting process and found that the intensive shearing not only influenced the solidification of the primary α-Al globules formed inside the slurry maker, but also the solidification process of the remaining liquid. It is therefore necessary

Foundation item: Projects (2006BA104B04-1; 2006BAE04B07-3) supported by the National Science and Technology Supporting Program of China; Project (2007KZ05) supported by the Science and Technology Supporting Project of Changchun City, China; Project supported by the "985 Project" of Jilin University, China

Corresponding author: ZHANG You-fa; Tel: +86-25-52090674; Fax: +86-25-52090658; E-mail: yfzhang@seu.edu.cn

DOI: 10.1016/S1003-6326(11)60706-1

and important to know the microstructure characteristics of all phases within the thixomolded AZ91D during heating, shearing, discharging, molding and cooling process.

2 Experimental

Commercial AZ91D chips and a JSW (Japan Steel Works) JLM220-MG prototype Thixomolder® were chosen to study microstructure characteristics and solidification behavior of thixomolded AZ91D during the forming process. The chemical compositions of AZ91D were checked by the ICP spectral analyzer and listed in Table 1, and the eutectic, solidus and liquidus temperatures of the experimental alloy were obtained to be 439, 502 and 595 °C by the curve of differential scanning calorimetry (DSC), studied by the previous work[7]. The main processing parameters for this experiment are as follows: barrel temperature 580−610 °C, shot velocity 2.09 m/s, screw rotation speed 168 r/min, injection pressure 30 MPa and mold temperature 230 °C. Cross section of the specimens was ground and polished, and then chemically etched in a 4% (volume fraction) solution of nitric acid in ethanol. Optical microscopy of OLYMPUS-PMG3 and laser microscopy of OLYPUS LEXT OLS3000 were selected to observe the optical microstructure. The phase composition of the alloy was checked using X-ray diffraction (D/max 2500pc Rigaku, Japan). Transmission electron microscopy (TEM) observations of thin foils were carried out using a JEM-2000EX instrument with an accelerating voltage of 200 kV. Thin foils with 3 mm in diameter were prepared by ion thinning. A selected area electron diffraction technique (SAD) in TEM was used for phase identification. Morphological and microchemical characterizations of polished surfaces were conducted by scanning electron microscopy (SEM) of JSM−5310 equipped with an energy dispersive X-ray spectrometer (EDAX).

Table 1 Chemical composition of AZ91D magnesium alloy (mass fraction, %)

Al	Zn	Mn	Si	Fe
8.30	0.54	0.14	0.011	0.0018
Cu	Ni	Others	Mg	
<0.01	<0.001	<0.001	Bal.	

3 Results

3.1 Typical microstructure of thixomolded AZ91D

The general microstructure of thixomolded AZ91D at room temperature is shown in Fig.1. It is seen that the microstructure contains some large phases (α_{un}) with different shapes (marked by arrows) and the solidified liquid alloy with deep color. The large phases can be divided into three kinds of morphologies in Fig.1, such as spherical (α_1), irregular (α_2), and with liquid alloy inside (α_3). In addition, it should be pointed out that there is the forth unmelted solid particles having little liquid inside, reported in the previous work[7]. The entrapped island in the forth particles is much smaller than that in α_3, and is signed as α_4 to separate from α_3.

Fig.2 provides the results of X-ray analysis of thixomolded AZ91D at different barrel temperatures. Obviously, temperature has great influence on solid

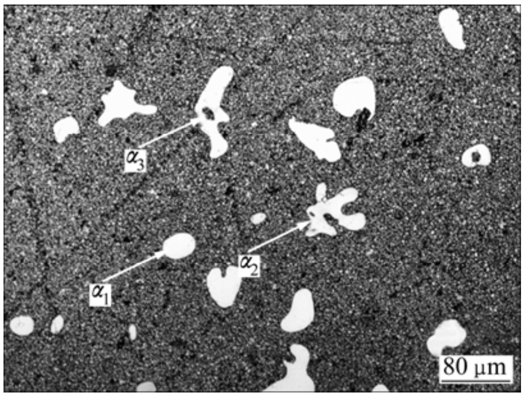

Fig.1 Typical microstructure of thixomolded AZ91D

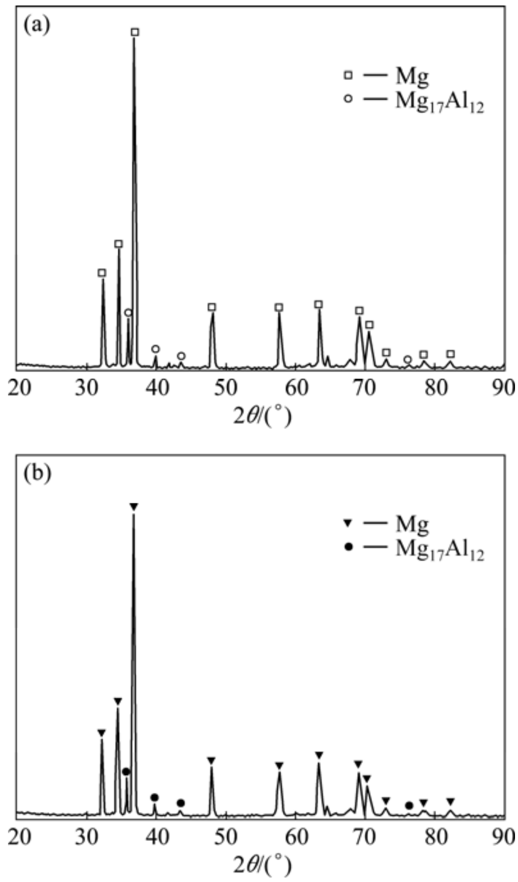

Fig.2 XRD patters of thixomolded AZ91D at different barrel temperatures: (a) 580 °C; (b) 600 °C

fraction, but doesn't change the phase composition. The alloy has two phases, including α-Mg with strong value in 2θ scanning and intermetallic compound $Mg_{17}Al_{12}$ having weak value in 2θ scanning. Compared with the Joint Committee on Powder Diffraction Standards (CPDS) card of α-Mg, it can be seen that the distribution of crystal surface of α-Mg in AZ91D is random and ruleless. $Mg_{17}Al_{12}$ also does not have special crystal surface.

In order to further understand the subtle details of thixomolded AZ91D, TEM observation is conducted, as shown in Fig.3. Fig.3(a) reveals that the white solid phase is solid solution of α-Mg by corresponding SAD diffraction pattern without containing precipitation of second phase. This regular and small α-Mg is considered primary grain, generating and growing during the solidification process of the remaining liquid alloy. According to the SAD diffraction pattern, the phase with deep color in both Fig.3(b) and Fig.3(c) represent intermetallic compound $Mg_{17}Al_{12}$ at different morphologies. Fig.3(b) shows the cross section of the fibrous compound while Fig.3(c) displays another cross section of the flake compound surrounding a α-Mg grain.

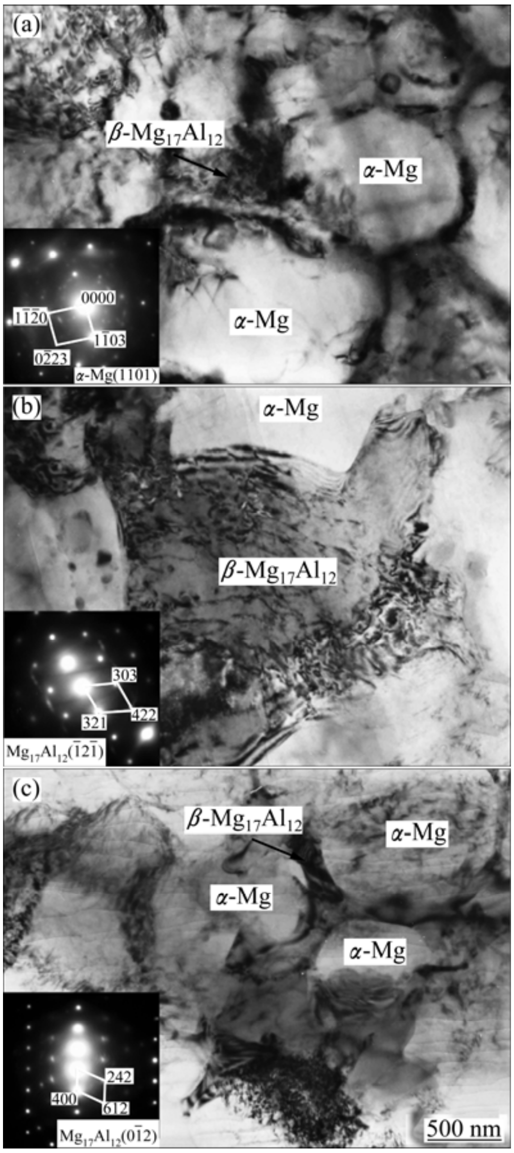

Fig.3 TEM microstructures of thixomolded AZ91D and corresponding SAD patterns: (a) α-Mg grain; (b) Cross section of $Mg_{17}Al_{12}$; (c) Another cross section of $Mg_{17}Al_{12}$

3.2 Unmelted solid particles

3.2.1 Spherical solid particles (α_1)

The microstructure and corresponding three-dimensional morphology of α_1 revealed in Fig.4 shows that this kind of particle considered the best solid phase within semisolid alloy, is in the size of 10−40 μm. They are spherical without any precipitation inside. Furthermore, the eutectic phase, showing deep color in Fig.4(b), distributes at the grain boundary and exhibits fine fibrous on the etched surface of the sample. In addition, some small solid particles of α-Mg are found with round shape and size of about 5 μm on the surface (marked by arrow).

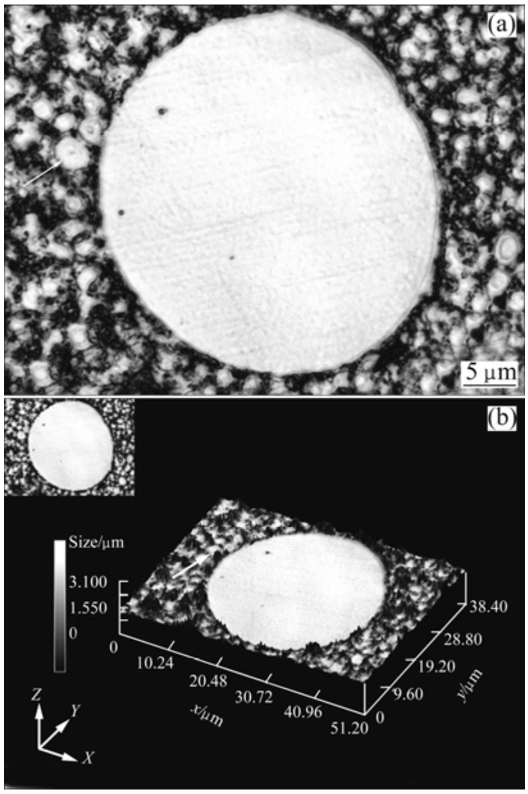

Fig.4 Microstructures of spherical solid particle: (a) 2-D morphology; (b) 3-D morphology by laser microscopy

3.2.2 Irregular solid particles (α_2)

As shown in Fig.1, lots of irregular solid particles with clean interior are presented within the microstructure of thixomolded AZ91D. As a common morphology of solid particles, α_2 is sometimes the main morphology occupying most of the solid particles, especially at high solid fraction or low shear rate.

According to the generation and transformation mechanism of non-dendritic solid particles, this morphology is thought to be the middle states of α_1 and α_3. Under the effect of shear, the arms of the particle may continuously bend till they combine together (Fig.5(a)), and at the same time, solid particles can collide with each other and then aggregate to form bigger irregular solid particle or entrap liquid alloy (Fig.5(b)). However, it should be mentioned that shear can destroy the aggregate into small spherical or irregular particles. In addition, some irregular solid phases may come out because of solidification when the semisolid alloy leaves the barrel into the shot sleeve without shear, but the size is relatively small compared with other α_2 for the small temperature gradient and short keeping time in the shot sleeve.

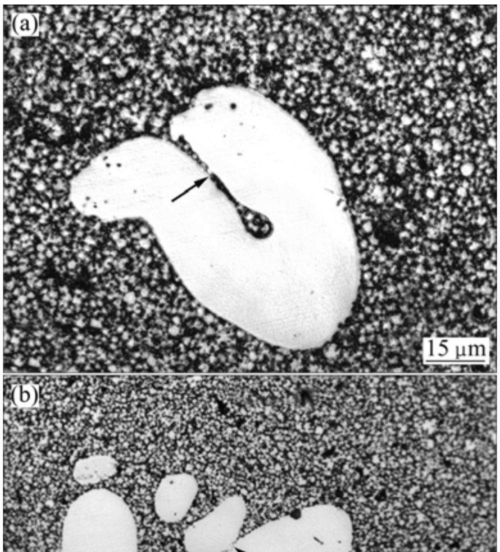

Fig.5 Formation of irregular solid particles: (a) Coalescence by bending of particle arm; (b) Coalescence by collision of particles (Arrows denote collision of two solid particles, which will induce big irregular particles.)

3.2.3 Particles with liquid alloy inside (α_3)

Displayed in Fig.6, microstructure of α_3 exhibits that the entrapped alloy is the same as the alloy outside α_3. The eutectic morphology revealed in Fig.6(b) is also the same as that in Fig.4(b). It can be concluded that α_3 mainly forms by agglomeration or the growth of small liquid pool or the arm bend of α_2 based on the recrystallization mechanism of solid particles.

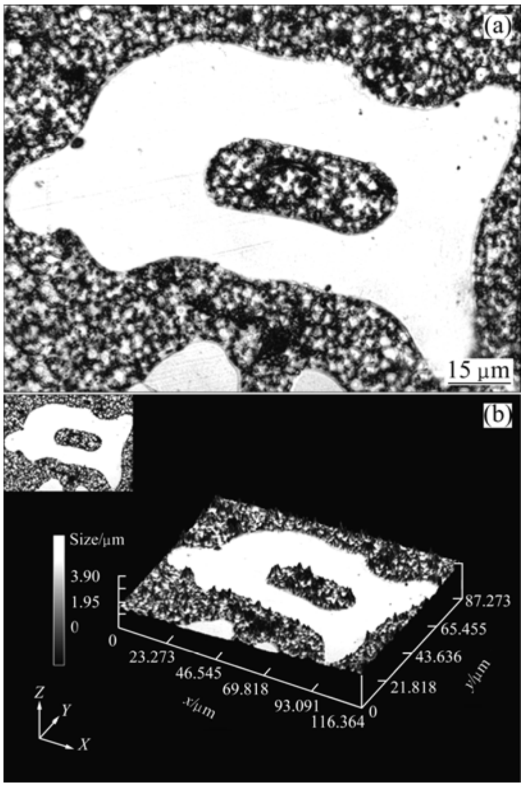

Fig.6 Microstructures of particles with liquid alloy inside: (a)2-D morphology; (b)3-D morphology by laser microscopy

3.2.4 Particles with liquid pool inside (α_4)

Liquid islands within the particles can be divided into two kinds of morphologies according to the entrapped volume. The big size in entrapped liquid is called liquid alloy, while the small size in entrapped liquid is liquid pool and the corresponding particle is called α_4. The number of liquid pools within α_4 is not sure, but they are small in the size of 5−20 μm and round shape, represented in Fig.7(a) and Fig.7(b). The liquid pool seems to be eutectic, having no small and round solid particle. It is confirmed that chemical segregation of Al in α-Mg which will melt at eutectic temperature exists in solid particles[6−7]. Then, forming and growing at the position under the effect of continuously diffusion of Al, the liquid pool moves with the mother solid particle and becomes solidification eutectic finally (Fig.7(c)), proved by EDAX (Fig.7(d)).

Transformation also happens to α_4, which can be initiative state of α_3 for the growth of entrapped pool. Obviously, the formation process of α_3 is melting but α_4 is entrapment. It should be pointed out that some entrapped liquid alloy may look like α_4 for the little entrapment.

3.3 Solidification microstructure of liquid phase in semisolid alloy

Solidification of the remaining liquid within the

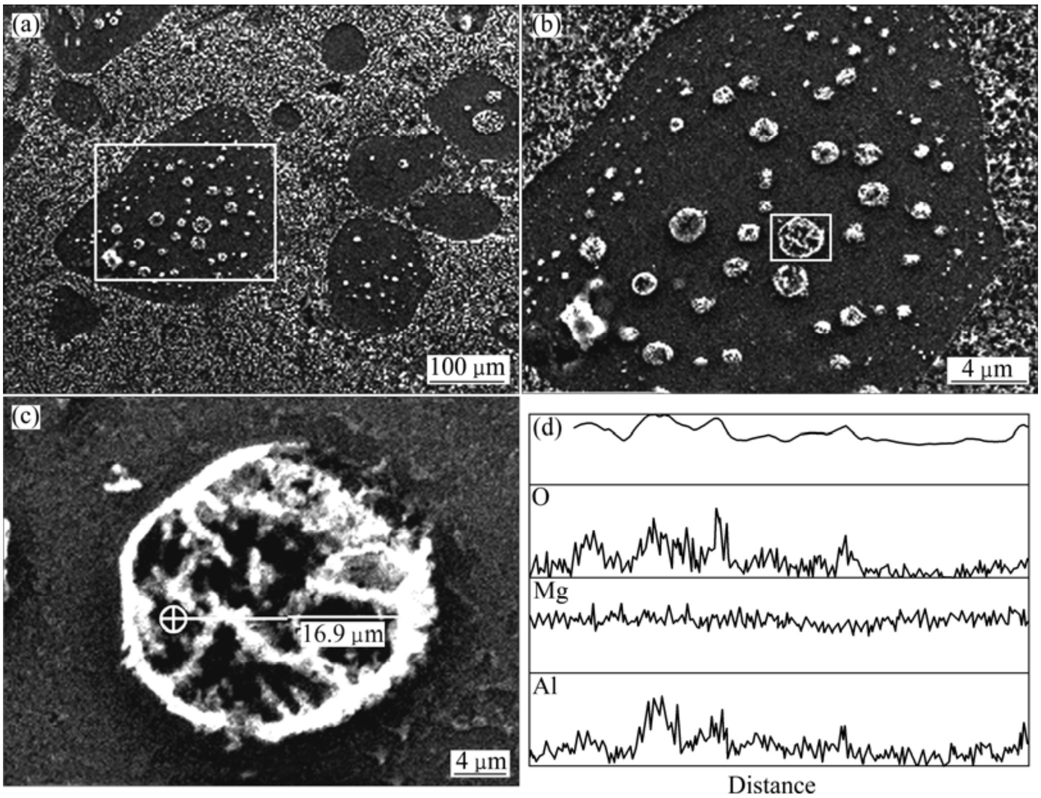

Fig.7 SEM morphologies of particles with liquid pool inside and EDAX spectra: (a) SEM image in low magnification; (b) SEM image in high magnification; (c) SEM image of liquid pool; (d) EDAX spectra

thixomolded AZ91D will start when the semisolid slurry leaves the barrel into the shot sleeve. Due to the low temperature of the sleeve, heterogeneous nucleation happens in the liquid alloy with dendrite structure under the condition of lack of shearing. However, this kind of particles as well as the particles of α_2, α_3 and α_4, may be fragmented when passing through the narrow nozzle and gate during the mold filling for the shear effect. During the following injection into the mold, the remaining liquid alloy will solidify to generate primary solid phase (α_{prim}) at first under a certain undercooling. Due to the prior intensive shearing, α_{prim} grows spherically with the uniform temperature and composition distribution, as typically marked by arrow in Fig.4. In addition, because of the enrichment of Al in the remaining liquid, the solute percentage in α_{prim} is more than that in α_{un}, and gets improvement with the solidification process by the equilibrium phase diagram.

4 Discussion

The solidification process of semisolid alloy is special and a little different from the liquid alloy because of the existence of unmelted solid phase. For AZ91D alloy in this study, main chemical compositions are Mg, Al and Zn without regard of the rest elements for the low content. According to the phase structure, Zn is similar to Al that can solve into α-Mg, or replace Al in the intermetallic compound of $Mg_{17}Al_{12}$ as $Mg_{17}(Al, Zn)_{12}$ or $Mg_{17}Al1_{1.5}Zn_{0.5}$[5]. Therefore, AZ91D alloy is considered a binary alloy of Mg-10% Al for this presentation according to its chemical composition. To the semisolid slurry with the volume fraction of φ_s, if it was supposed that the solution content of Al in α-Mg keeps 3% (solution degree at 200 °C)[6], the content of Al in liquid phase $\varphi(Al_l)$ is obtained from the following equation:

$$\varphi(\mathrm{Al_l}) = \frac{0.1 - 3\%\varphi_s}{1-\varphi_s} \times 100\% \tag{1}$$

Theoretically, when φ_s is lower than 27.8% ($\varphi(Al_l)$ is lower than 12.7%, the maximum solution degree of Al in Mg (Eq.(1)), the solidified microstructure of semisolid Mg-10% Al alloy should be composed of α_{un}, α_{prim} and secondary β-$Mg_{17}Al_{12}$ (β_{II}). Similarly, the alloy contains α_{un}, α_{prim}, β_{II} and eutectic when the fraction is higher than 27.8% and will only have α_{un} and eutectic at the volume fraction of 76.1%. However, actually, the Al content in the remaining liquid phase of semisolid AZ91D increases with the solidification process and results in eutectic reaction once the content reaches the maximum solution degree of Al in Mg. Therefore, the microstructure of thixomolded AZ91D at room temperature is composed of α_{un}, α_{prim}, β_{II} and eutectic if its solid fraction is lower than 76.1%.

The solid particles of α_{un} and α_{prim} are different in the generation, size, morphology and chemical composition. The generation of α_{un} is based on the recrystallization mechanism while α_{prim} is controlled by crystallization theory. Furthermore, α_{un} has big size and can have four kinds of morphologies such as spherical (α_1), irregular (α_2), with liquid alloy inside (α_3) and with liquid pool inside (α_4). Compared with α_{un}, α_{prim} is rounder and smaller with enrichment of Al. In general view of four kinds of α_{un}, α_2 and α_4 are the middle states of α_1 and α_3, α_4 and α_3 can break into α_2 and become α_1 at the end. Therefore, α_1 is considered the final morphology of the rest three kinds. When the solid fraction and shear effect come to an ideal combination, the perfect semisolid alloy with small and spherical solid phase can be achieved. And then the products using this kind of slurry will certainly obtain the best quality and properties if the processing parameters and mold design are reasonable.

Due to the excellent cooling effect of metallic die block, large cooling rate (about 10^3 K/s) is attained and makes nucleation take place at a high nucleation rate in the remaining liquid alloy of thixomolded AZ91D. The nuclei compete against each other to grow till instability occurs, which prevents them from irregular grains by dendritically developing. Finally, controlled by undercooling, the fine small spherical α_{prim} with size of about 5 μm is produced, while the size of α_{un} is usually bigger than 10 μm and mainly influenced by solid fraction and shearing. It is believed that the growth of α_{prim} will complete before the appearance of instability. The Mullins-Sekerka instability theory points out that a spherical crystal growing in liquid alloy will be morphologically unstable when its size reaches the following critical value R_c[13]:

$$R_c = \frac{2(\gamma_{sl}/L_v)(7+4k_s/k_l)}{\Delta T/T_m} \tag{2}$$

where T_m and ΔT are the melting point and the undercooling: k_s and k_l are thermal conductivities of liquid and solid Mg at the melting point temperature; γ_{sl} is the interfacial energy at the solid/liquid interface; and L_v is the latent heat of fusion per unit volume of the solid. The physical meaning in above equation and parameter values of pure magnesium are collected in Table 2. By substituting the corresponding values into the above equation, the critical value R_c is

$$R_c = \frac{4.92}{\Delta T} \tag{3}$$

Table 2 Thermochemical and physical properties of solid and liquid magnesium at melting point[12−14]

Parameter	Value
Melting point, T_m/K	923
Density of liquid magnesium at T_m, ρ_l/(g·cm^{-3})	1.584
Volume change from solid to liquid at T_m, ΔV_m/%	4.2
Density of solid magnesium at T_m, ρ_s/(g·cm^{-3})	1.653
Thermal conductivity of liquid magnesium at T_m, k_l/(W·m^{-1}·K^{-1})	78
Thermal conductivity of solid magnesium at T_m, k_s/(W·m^{-1}·K^{-1})	130
Latent heat of fusion of magnesium, L_m/(kJ·mol^{-1})	8.954
Latent heat of fusion of magnesium, L_v/(GJ·m^{-3})	0.59
Solid-liquid interfacial free energy of magnesium, γ_{sl}/(J·m^{-3})	0.115

It is clear that the critical value R_c is sensitive to the undercooling ΔT. In this study, it is difficult in direct measurement of the undercooling in the die cavity. Assuming a similar level of 1−2 K as the work of HITCHCOCK et al[12], the primary solid particle can grow stably to the diameter of 4.92−9.84 μm or larger according to the above equation. Actually, the average α_{prim} particle size has been investigated to be about 5 μm in diameter, indicating that the α_{prim} particle is close to its spherical growth instability.

Giving a local solidification time of about 1 s, the growth rate for α_{prim} is 2.5 μm/s. If assuming the same growth velocity of grain formation in the shot sleeve, the solid particles will lose their stability for spherical developing after 1s and can reach the size of 15 μm after the discharge time of 3 s. Therefore, the formation of this kind of dendritical solid particle becomes a significant part of the small irregular solid phase without entrapped liquid alloy except the formation by collision and agglomeration.

5 Conclusions

1) Typical microstructure of thixomolded AZ91D is composed of α-Mg and β-$Mg_{17}Al_{12}$. In general view, the phases are characterized with large α_{un}, fine round α_{prim} with the size of about 5 μm and eutectic exhibiting fibrous or well-branched flake. α_{un} and α_{prim} are different in the generation, size, morphology and chemical composition.

2) According to the morphology and generation mechanism, α_{un} can be classified into four kinds, such as spherical (α_1), irregular (α_2), entrapping liquid alloy inside (α_3) and entrapping pool inside (α_4). The final and best solid particle is thought to be α_1 having the size of 10−40 μm because the others can become α_1 under the

effect of heating, shearing, collision, agglomeration or fragmentation.

3) α_{prim} nucleates and grows in the remaining liquid alloy until instability growth. This kind of solid particle, controlled by undercooling, is round and small with enrichment of Al compared with α_{un}. The size could be 4.92−9.84 μm at the undercooling of 1−2 K.

Acknowledgments

The authors are very grateful to Professor YU Xin-quan and Professor CHEN Feng who are School of Materials Science and Engineering, Southeast University, for helpful discussion.

References

[1] MORDIKE M L, EBERT T. Magnesium properties-applications-potential [J]. Mater Sci Eng A, 2001, 302: 37−45.

[2] SPENCER D B, MEHRABIAN R, FLEMINGS M C. Rheological behavior of Sn-15pct Pb in the crystallization range [J]. Metall Trans, 1972, 3(7): 1925−1932.

[3] FAN Z. Semisolid metal processing [J]. Int Mater Rev, 2002, 47: 49−85.

[4] ZHANG Y F, LIU Y B, CAO Z Y, ZHANG Q Q, ZHANG L. Mechanical properties of thixomolded AZ91D magnesium alloy [J]. J Mater Process Tech, 2009, 29: 1375−1384.

[5] CZERWINSKI F. ZIELINSKA A, PINET P J, OVERBEEKE J. Correlating the microstructure and tensile properties of a thixomolded AZ91D magnesium alloy [J]. Acta Mater, 2001, 49: 1225−1235.

[6] CZERWINSKI F. The microstructural development of Mg-9 pct Al-1 pct Zn alloy during shot molding [J]. Metall Mater Trans A, 2002, 33: 2963−2972.

[7] ZHANG Y F, LIU Y B, ZHANG Q Q, CAO Z Y, CUI X P, WANG Y. Microstructural evolution of thixomolded AZ91D magnesium alloy with process parameters variation [J]. Mater Sci Eng A, 2007, 444: 251−256.

[8] ZHANG You-fa, LIU Yong-bing, CAO Zhan-yi. Microstructure transformation of deformed AZ91D during isothermal holding [J]. Transactions of Nonferrous Metals Society of China, 2010, 20(1): 14−21.

[9] TSUKEDA T, TAKEYA K, SAITO K, KUBO H. Mechanical and metallurgical properties of injection molded AZ91D magnesium alloy [J]. J Japan Inst Light Metals, 1999, 49: 287−290.

[10] CHEN J Y, FAN Z. Modelling of rheological behavior of semisolid metal slurries [J]. Mater Sci Tech, 2002, 18: 237−267.

[11] GUAN R, CHEN L, LI J, WANG F. Dynamical solidification behaviors and metal flow during continuous semisolid extrusion process of AZ31 alloy [J]. J Mater Sci Technol, 2009, 25(3): 395−400.

[12] HITCHCOCK M, WANG Y, FAN Z. Secondary solidification behaviour of the Al-Si-Mg alloy prepared by the rheo-diecasting process [J]. Acta Mater, 2007, 55: 1589−1598.

[13] MULLINS W W, SEKERKA R F. Morphological stability of a particle growing by diffusion or heat flow [J]. J Appl Phys, 1963, 34: 323−329.

[14] CZERWINSKI F. Magnesium injection molding [M]. New York: Springer Verlag, 2008: 19−21.

触变注射成形 Mg-9%Al-1%Zn 合金组织特性和凝固行为

张友法[1]，刘勇兵[2]，曹占义[2]

1. 东南大学 材料科学与工程学院，江苏省先进金属材料高技术研究重点试验室，南京 211189;
2. 吉林大学 材料科学与工程学院，汽车材料教育部重点实验室，长春 130022

摘　要：为了研究触变注射成形 AZ91D 合金中固相颗粒的形貌演变和液相的凝固行为，对该合金的组织和凝固行为进行了试验观察和理论分析。典型触变注射成形 AZ91D 合金由 α-Mg 和 β-$Mg_{17}Al_{12}$ 两相构成，α-Mg 相又可分为未熔固相和初生固相。未熔固相主要有形貌较为接近球状的固相、形貌不规则的固相、内部含有小液池的固相以及包裹液相的固相 4 种形貌。形貌不规则的固相被认为是球状固相和包裹液相的固相的中间发展形貌，内部含有小液池的固相可能是包裹液相的固相的初级形貌，包裹液相的固相则可能发生破裂形成不规则固相，最终发展成球状固相。球状固相被认为是最理想的也是最终的固相形貌。初生固相在液相合金中形核并长大，直至有不稳定长大行为发生为止，较为细小、圆整，主要受冷却速率的影响。Mg-Al 合金二元相图的分析结果与试验观察到的组织相吻合。

关键词：触变注射；AZ91D；固相颗粒；凝固行为

(Edited by LI Xiang-qun)